



## Research paper

## Clathrocin, hymenidin and oroidin, and their synthetic analogues as inhibitors of the voltage-gated potassium channels



Nace Zidar<sup>a</sup>, Aleš Žula<sup>a</sup>, Tihomir Tomašič<sup>a</sup>, Marc Rogers<sup>b,1</sup>, Robert W. Kirby<sup>b,1</sup>, Jan Tytgat<sup>c</sup>, Steve Peigneur<sup>c</sup>, Danijel Kikelj<sup>a</sup>, Janez Ilaš<sup>a,\*\*</sup>, Lucija Peterlin Mašič<sup>a,\*</sup>

<sup>a</sup> University of Ljubljana, Faculty of Pharmacy, Aškerčeva cesta 7, 1000 Ljubljana, Slovenia

<sup>b</sup> Xention Limited, Iconix Park, London Road, Pampisford, Cambridge CB22 3EG, UK

<sup>c</sup> University of Leuven (KU Leuven), Toxicology & Pharmacology, O&N2, PO Box 922, Herestraat 49, 3000 Leuven, Belgium

## ARTICLE INFO

## Article history:

Received 18 January 2017

Received in revised form

3 August 2017

Accepted 4 August 2017

Available online 7 August 2017

## Keywords:

Voltage-gated potassium channel

K<sub>v</sub>1

Modulator

Inhibitor

Clathrocin

Oroidin

Hymenidin

## ABSTRACT

We have prepared three alkaloids from the *Agelas* sponges, clathrocin, hymenidin and oroidin, and a series of their synthetic analogues, and evaluated their inhibitory effect against six isoforms of the K<sub>v</sub>1 subfamily of voltage-gated potassium channels, K<sub>v</sub>1.1–K<sub>v</sub>1.6, expressed in Chinese Hamster ovary (CHO) cells using automated patch clamp electrophysiology assay. The most potent inhibitor was the (*E*)-*N*-(3-(2-amino-1*H*-imidazol-4-yl)allyl)-4,5-dichloro-1*H*-pyrrole-2-carboxamide (**6g**) with IC<sub>50</sub> values between 1.4 and 6.1 μM against K<sub>v</sub>1.3, K<sub>v</sub>1.4, K<sub>v</sub>1.5 and K<sub>v</sub>1.6 channels. All compounds tested displayed selectivity against K<sub>v</sub>1.1 and K<sub>v</sub>1.2 channels. For confirmation of their activity and selectivity, compounds were additionally evaluated in the second independent system against K<sub>v</sub>1.1–K<sub>v</sub>1.6 and K<sub>v</sub>10.1 channels expressed in *Xenopus laevis* oocytes under voltage clamp conditions where IC<sub>50</sub> values against K<sub>v</sub>1.3–K<sub>v</sub>1.6 channels for the most active analogues (e.g. **6g**) were lower than 1 μM. Because of the observed low sub-micromolar IC<sub>50</sub> values and fairly low molecular weights, the prepared compounds represent good starting points for further optimisation towards more potent and selective voltage-gated potassium channel inhibitors.

© 2017 Elsevier Masson SAS. All rights reserved.

## 1. Introduction

Voltage-gated potassium (K<sub>v</sub>) channels are molecular complexes responsible for initiation and propagation of electrical impulses in excitable cells such as neurons, myocytes and endocrine cells, as well as for the transduction of signals in non-excitabile cells such as immune cells. K<sub>v</sub> channels are homo- or heterotetrameric proteins composed of four circularly arranged α subunits that form an ion conducting pore and contain voltage-sensing domains, and one or more supplementary β subunits [1,2]. K<sub>v</sub> channels are a very large and diverse group of proteins and represent the largest branch of the potassium channel family. In humans, there are currently 40 known genes encoding K<sub>v</sub> channel α subunits and

based on their sequence homology and function, K<sub>v</sub> channels can be divided into 12 major subfamilies (K<sub>v</sub>1–12). Additionally, each of the 12 subfamilies is composed of several members that differ in their structures, biophysical profile and expression patterns in different tissue types which facilitate their different biological roles [3]. There are currently eight known pore-forming α subunits of the K<sub>v</sub>1 subfamily (K<sub>v</sub>1.1–K<sub>v</sub>1.8), among which K<sub>v</sub>1.1 and K<sub>v</sub>1.2 channels are mainly expressed in the central nervous system (CNS), K<sub>v</sub>1.3 channels are typical for T and B lymphocytes and macrophages, the rapidly inactivating K<sub>v</sub>1.4 channels can be found in CNS, skeletal muscle, heart and pancreatic islets, K<sub>v</sub>1.5 channels are located in cardiac myocytes, immune cells and vascular smooth muscle, while the K<sub>v</sub>1.6 channels are expressed in spinal cord, CNS, astrocytes and artery smooth muscle. The high expression of K<sub>v</sub>1.7 and K<sub>v</sub>1.8 channels is typical for the heart, skeletal muscle and CNS [2,4].

The loss- and gain-of-function mutations - the channelopathies - of the K<sub>v</sub>1 channel subfamily have been associated with various pathological phenotypes which highlight the potential of K<sub>v</sub>1 channels as promising drug targets [3,4]. Modulators of K<sub>v</sub>1.1 and K<sub>v</sub>1.2 channels have been described as potential targets for the

\* Corresponding author.

\*\* Corresponding author.

E-mail addresses: [Janez.Ilas@ffa.uni-lj.si](mailto:Janez.Ilas@ffa.uni-lj.si) (J. Ilaš), [Lucija.PeterlinMasic@ffa.uni-lj.si](mailto:Lucija.PeterlinMasic@ffa.uni-lj.si) (L.P. Mašič).

<sup>1</sup> Current address: Metrion Biosciences Limited, Babraham Research Campus, Cambridge, CB22 3AT, UK.

treatment of epilepsy and neuropathic pain [5,6], inhibitors of  $K_v1.3$  channels exert immunosuppressive effects and have potential for the treatment of various autoimmune diseases [7–9], blockers of  $K_v1.5$  channels are in development as antiarrhythmics [10–12], while  $K_v1.4$ ,  $K_v1.6$ ,  $K_v1.7$  and  $K_v1.8$  channels have so far a less well defined therapeutic relevance.

Among the  $K_v1$  subfamily, in recent years, the  $K_v1.3$  channel has arguably received the most scientific attention as a drug target. Efflux of  $K^+$  ions through  $K_v1.3$  channels is necessary to repolarize the membrane potential in immune cells. A negative membrane potential is required to allow activation of calcium release-activated channels (CRAC) channels upon a new depolarization. As such,  $K_v1.3$  channels indirectly create a driving force for the entry of  $Ca^{2+}$  ions through CRAC channels. The resultant influx of  $Ca^{2+}$  is necessary for the translocation of nuclear factors which results in T cell activation, proliferation and inflammatory cytokine secretion. Thus, selective  $K_v1.3$  inhibition could be regarded as a novel approach for the treatment of autoimmune diseases such as multiple sclerosis, rheumatoid arthritis and psoriasis [3,4,13].

There are two main binding sites for small-molecules on  $K_v1$  channels reported in the literature: the inner-pore site and a side-pocket cavity [14]. Since the sequence of the inner pore is well conserved among the  $K_v1$  family, the majority of blockers that bind to this site are not very selective, e.g. 4-aminopyridine (4-AP, Fig. 1) and tetrabutylammonium (TBA, Fig. 1). Reasonable  $K_v1.3$  selectivity has been reported for correolide (Fig. 1) [15], and for PAP-1 (Fig. 1) [16], a member of the phenoxyalkoxy-psoralen family, which displays a 2 nM  $IC_{50}$  value against  $K_v1.3$  and a 4- to 20-fold selectivity against  $K_v1.1$ ,  $K_v1.2$ ,  $K_v1.4$ ,  $K_v1.5$  and  $K_v1.6$  channels.

Despite tremendous research efforts in the  $K_v$  channel drug discovery field the therapeutic potential of  $K_v$  channels remains underexploited. The main problems are (i) the lack of structural channel data and the information on the exact binding site of compounds, (ii) low structural diversity of leads, (iii) poor gene family selectivity and/or (iv) unfavourable physicochemical properties of compounds, which result in non-optimal efficacy and toxicity issues. However, recent advances in crystallisation of  $K_v$  channels [17–19] and new *in silico* studies [14] are increasing our knowledge of their structure and function. Additionally, over the last few years development of new reliable high- and medium throughput screening methods such as the Sophion QPatch 48 automated patch-clamp electrophysiology system have helped accelerate the drug discovery process for ion channel modulators [4].

Marine organisms, such as sponges, fish, cone snails, cnidarians and sea anemones, are important sources of various bioactive compounds that are used in their native environment to capture prey or function as defence against predators [20]. Alkaloids isolated from marine sponges *Agelas* sp., clathrocin, hymenidin and oroidin (Fig. 2), and their synthetic analogues, have been shown to possess modulatory activities on voltage-gated sodium ( $Na_v$ ) channels [21–23], but so far their activity on  $K_v$  channels has not been reported. However, complex marine compounds isolated from

other species of marine sponges (acredinones and crambescins) have recently shown inhibitory activity against  $K_v$  channels [24,25]. Because of their relatively simple structures and lead-like properties, clathrocin, hymenidin and oroidin represent interesting starting compounds for medicinal chemistry optimisation of their pharmacological properties.

In our study, we have prepared clathrocin, hymenidin and oroidin, and a series of their synthetic analogues, and evaluated their  $K_v1$  channel inhibitory activity against six different human  $K_v1$  channel subtypes expressed in Chinese hamster ovary cells (CHO cells) using automated patch clamp electrophysiology. All of the prepared compounds were evaluated against  $K_v1.3$  channels, and active inhibitors also against  $K_v1.1$ ,  $K_v1.2$ ,  $K_v1.4$ ,  $K_v1.5$  and  $K_v1.6$  channels. In addition to the automated patch clamp electrophysiology, compounds were also studied in the second, independent test system under voltage clamp conditions against  $K_v1.1$ - $K_v1.6$  and  $K_v10.1$  channels expressed in *Xenopus laevis* oocytes. Based on the inhibitory activities, structure-activity relationship (SAR) of this new structural class of voltage-gated potassium channel modulators was studied.

## 2. Results and discussion

### 2.1. Design

We have prepared clathrocin, hymenidin and oroidin (Fig. 2), and evaluated their inhibitory effect against  $K_v1.1$ - $K_v1.6$  channels. With the aim of improving the activities and/or stabilities of the natural alkaloids, we have designed two structural classes of their analogues, (*E*)-*N*-(3-(2-amino-1*H*-imidazol-4-yl)allyl)carboxamides **I** and *N*-(3-(2-amino-1*H*-imidazol-4-yl)propyl)carboxamides **II** (Fig. 2).

In the type **I** series we decided to retain the (*E*)-4-(3-aminoprop-1-en-1-yl)-1*H*-imidazol-2-yl motif on the left-hand side of the molecules and to replace the right-hand side pyrrol-2-yl (**6a**, Table 1), 4-bromopyrrol-2-yl (**6b**, Table 1), and 4,5-dibromopyrrol-2-yl (**6c**, Table 1) groups that are present in natural alkaloids, with other substituted pyrrol-2-yl (**6d-g**, Table 1), indol-2-yl (**6h-k**, Table 1), indolin-2-yl (**6l**, Table 1), pyridin-3-yl (**6m**, Table 1), and piperidin-4-yl (**6n-o**, Table 1) groups. In this way we examined the influence of different size, polarity and/or acid/base properties of the right-hand side groups on the biological activity. Additionally, with piperidine derivatives **6n** and **6o**, we examined if the aromaticity of the right-hand side groups is important for  $K_v1$  inhibitory activity.

In the type **II** series we aimed at increasing the chemical stability of compounds by eliminating the potentially reactive double bond in the central part of the molecules and replacing it with the saturated propylene group. In this way, we also studied the influence of increased flexibility and conformational freedom of molecules on the  $K_v1$  inhibitory activity. Analogously to the type **I** series, in addition to the analogue with naturally occurring 4,5-dibromopyrrol-2-yl group (**14a**, Table 1), we have prepared

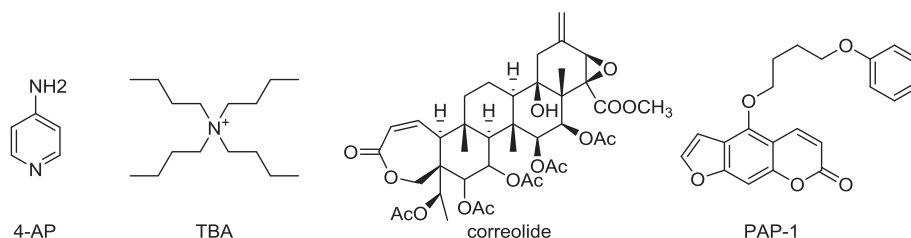
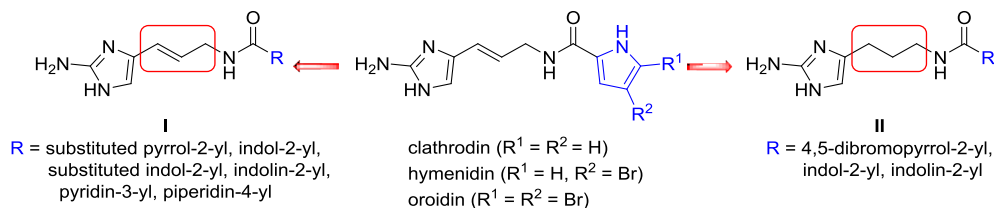


Fig. 1. Structures of the unselective  $K_v$  channel inhibitors (4-AP, TBA) and  $K_v1.3$  selective inhibitors (correolide, PAP-1).



**Fig. 2.** Agelas alkaloids clathrocin, oroidin and hymenidin, and two structural classes of the designed analogues, (*E*)-*N*-(3-(2-amino-1*H*-imidazol-4-yl)allyl)carboxamides **I** and *N*-(3-(2-amino-1*H*-imidazol-4-yl)propyl)carboxamides **II**.

analogues with bulkier indol-2-yl (**14b**, Table 1) and indolin-2-yl (**14c**, Table 1) groups on the right-hand side of the molecules.

## 2.2. Chemistry

Type **I** compounds were prepared according to Fig. 3. First, pyridine (**1**) was acylated with benzyl chloroformate, followed by reduction with sodium borohydride to give *N*-Cbz-1,2-dihydropyridine (**2**). Reaction of compound **2** with *N*-Boc-guanidine in the presence of bromine afforded two regioisomers **3a** and **3b**, which after deprotection yielded amine **4** [26]. Final compounds **6a–o** were prepared by TBTU-promoted coupling of amine **4** and the appropriate carboxylic acids with good regioselectivity.

Compounds **14a–c** were prepared as depicted in Fig. 4. First, L-ornithine (**7**) was Boc-diprotected to yield compound **8**, which was then converted to Weinreb amide **9**. A second Boc protecting group was introduced to  $\delta$  position of **9** to yield compound **10**, followed by the reduction of **10** to give aldehyde **11**. Aldehyde **11** was Boc-deprotected with gaseous HCl and then formation of a 2-aminoimidazole ring was achieved using cyanamide to yield saturated amine **13** [26]. TBTU was used for the coupling between amine **13** and the appropriate carboxylic acids with good regioselectivity to yield amides **14a–c**.

## 2.3. Inhibitory activity of compounds against K<sub>v</sub>1 channels

Altogether 18 compounds were prepared and evaluated for their inhibitory activities against different K<sub>v</sub>1 channel isoforms. The channels were heterologously expressed in two different expression systems, mammalian CHO cells and *Xenopus laevis* oocytes. For the analysis of compounds against K<sub>v</sub>1.1–K<sub>v</sub>1.6 isoforms expressed in CHO cells, automated patch clamp electrophysiology assay was used. The compounds were additionally analysed on K<sub>v</sub>1.1–K<sub>v</sub>1.6 and K<sub>v</sub>10.1 channels expressed in *Xenopus laevis* oocytes under voltage clamp conditions. The results are expressed as IC<sub>50</sub> values (the concentration of compound that inhibits potassium channel activity by 50%) or as percent inhibition at the 1  $\mu$ M test concentration and are presented in Tables 1 and 2, and Table 1S of the Supplementary information.

Automated patch clamp electrophysiology assay was performed on the QPatch48 HT system (Sophion, Denmark) using whole cell configuration mode. The potency of compounds against the K<sub>v</sub>1 channel subtypes was determined from concentration–response relationships established by cumulatively applying four escalating concentrations of test compound to a cell. Two-electrode voltage-clamp recordings were performed using a GeneClamp 500 amplifier (Molecular Devices, Sunnyvale, California, USA) controlled by a pClamp data acquisition system (Axon Instruments, USA). For details see Experimental section.

The results of the automated patch clamp electrophysiology are presented in Table 1 and can be summarised as follows. Some of the compounds, e.g. **6b**, **6c**, and **6g**, exhibited promising inhibitory activities against different K<sub>v</sub>1 channel isoforms in the low

micromolar range, with moderate isoform selectivity. The observed potencies were generally higher for K<sub>v</sub>1.3, K<sub>v</sub>1.4, and K<sub>v</sub>1.6 channels, while none of the compounds were active against K<sub>v</sub>1.1 and K<sub>v</sub>1.2 channels. By comparing the biological results for alkaloids clathrocin (**6a**), hymenidin (**6b**), and oroidin (**6c**) it can be seen, that the introduction of bromo substituents to the pyrrole ring on the right-hand side of the molecules increases the inhibitory activity against K<sub>v</sub>1 channels. Clathrocin (**6a**) with an unsubstituted pyrrole-2-yl group was inactive against all K<sub>v</sub>1 channel isoforms, while hymenidin (**6b**) and oroidin (**6c**) displayed inhibitory activities against K<sub>v</sub>1.3–K<sub>v</sub>1.6 isoforms. The observed differences in potencies can be rationalised either by the increase in volume and lipophilicity because of the additional bromo substituent, or by the electron-withdrawing effects of bromine which increases the acid properties of the pyrrole NH and thus makes it a better H-bond donor. Interestingly, hymenidin (**6b**) with 4-bromopyrrol-2-yl group (IC<sub>50</sub> for K<sub>v</sub>1.3 = 2.5  $\mu$ M, IC<sub>50</sub> for K<sub>v</sub>1.5 = 7.6  $\mu$ M, and IC<sub>50</sub> for K<sub>v</sub>1.6 = 3.7  $\mu$ M) was generally more potent than oroidin (**6c**) with 4,5-dibromopyrrol-2-yl group (IC<sub>50</sub> for K<sub>v</sub>1.3 = 4.7  $\mu$ M, IC<sub>50</sub> for K<sub>v</sub>1.5 = 2.1  $\mu$ M, and IC<sub>50</sub> for K<sub>v</sub>1.6 = 4.9  $\mu$ M). The only exception was the K<sub>v</sub>1.4 channel where oroidin (IC<sub>50</sub> = 2.1  $\mu$ M) was more potent than hymenidin (IC<sub>50</sub> = 5.3  $\mu$ M).

In the type **I** series of clathrocin analogues, the most potent inhibitor was the 4,5-dichloropyrro-2-yl derivative **6g**, with IC<sub>50</sub> values of 1.4  $\mu$ M, 1.5  $\mu$ M, and 1.6  $\mu$ M against K<sub>v</sub>1.3, K<sub>v</sub>1.4, and K<sub>v</sub>1.6 channels, respectively. This indicates that slightly smaller chlorine atoms are more optimal for increasing the binding affinity than bromine atoms. Compounds **6h–k** with indole groups on the right-hand side of the molecules were less potent than the pyrrole analogues. Among the indole derivatives, the two most potent inhibitors were the 5-fluoroindole **6i** (IC<sub>50</sub> for K<sub>v</sub>1.4 = 8.8  $\mu$ M, IC<sub>50</sub> for K<sub>v</sub>1.6 = 7.9  $\mu$ M), and the 5-chloroindole **6j** (IC<sub>50</sub> for K<sub>v</sub>1.3 = 9.0  $\mu$ M). Compound **6j** was interesting also because of its selectivity as it was inactive against K<sub>v</sub>1.1, K<sub>v</sub>1.2 and K<sub>v</sub>1.5 channels, and only weakly active against K<sub>v</sub>1.4 (IC<sub>50</sub> = 17  $\mu$ M) and K<sub>v</sub>1.6 (IC<sub>50</sub> = 24  $\mu$ M) channels. Compounds with indolin-2-yl (**6l**), pyridin-3-yl (**6m**), and piperidin-4-yl (**6n–o**) groups on the right-hand side of the molecules were inactive against all of the tested K<sub>v</sub>1 isoforms. Similarly, compounds of the type **II** series (**14a–c**) with the reduced double bond in the central part of the molecules did not display any activity against K<sub>v</sub>1 channels.

The results of the voltage clamp experiments on K<sub>v</sub> channels expressed in *X. laevis* oocytes are presented in Table 1S (Supplementary information) and Table 2. First, the initial selectivity profiling was performed for all 18 compounds against K<sub>v</sub>1.1–K<sub>v</sub>1.6 and K<sub>v</sub>10.1 channels at 1  $\mu$ M concentration. The activities are presented in Table 1S as percent inhibition of potassium channel currents. Based on these results, five most potent compounds were selected for the determination of IC<sub>50</sub> values on K<sub>v</sub>1.3, K<sub>v</sub>1.4 and K<sub>v</sub>1.6 channels (Table 2). From the data presented in Tables 1S and 2 a similar trend can be observed as for the automated patch clamp experiments. Clathrocin (**6a**) with no substituents on the pyrrole ring was inactive against all of the tested K<sub>v</sub> isoforms. The

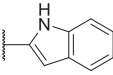
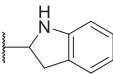
**Table 1**

Inhibitory activities of (*E*)-*N*-(3-(2-amino-1*H*-imidazol-4-yl)allyl)carboxamides **6a-o** and *N*-(3-(2-amino-1*H*-imidazol-4-yl)propyl)carboxamides **14a-c** on K<sub>v</sub>1.1-K<sub>v</sub>1.6 channels expressed in CHO cells.

Compd.	R	IC <sub>50</sub> (μM) <sup>a</sup>					
		K <sub>v</sub> 1.1	K <sub>v</sub> 1.2	K <sub>v</sub> 1.3	K <sub>v</sub> 1.4	K <sub>v</sub> 1.5	K <sub>v</sub> 1.6
<b>6a</b> clathrocin		n.a. <sup>b</sup>	n.a.	n.a.	n.a.	n.a.	n.a.
<b>6b</b> hymenidin		n.a.	n.a.	2.5 ± 0.1	5.3 ± 0.5	7.6 ± 1.7	3.7 ± 1.0
<b>6c</b> oroidin		n.a.	20 ± 14	4.7 ± 1.3	2.1 ± 0.4	16 ± 10	4.9 ± 1.6
<b>6d</b>		n.a.	n.a.	25 ± 3	12 ± 4	n.a.	11 ± 4
<b>6e</b>		n.a.	n.a.	17 ± 5	12 ± 3	n.a.	29 ± 2
<b>6f</b>		n.a.	n.a.	25 ± 8	15 ± 2	n.a.	17 ± 4
<b>6g</b>		n.a.	n.a.	1.4 ± 0.1	1.5 ± 0.5	6.1 ± 1.9	1.6 ± 0.2
<b>6h</b>		n.a.	n.a.	21 ± 3	13 ± 2	n.a.	14 ± 3
<b>6i</b>		n.a.	n.a.	14 ± 3	8.8 ± 2.8	n.a.	7.9 ± 1.4
<b>6j</b>		n.a.	n.a.	9.0 ± 0.7	17 ± 5	n.a.	24 ± 4
<b>6k</b>		- <sup>c</sup>	—	n.a.	—	—	—
<b>6l</b>		—	—	n.a.	—	—	—
<b>6m</b>		—	—	n.a.	—	—	—
<b>6n</b>		—	—	n.a.	—	—	—
<b>6o</b>		—	—	n.a.	—	—	—
<b>14a</b>		—	—	n.a.	—	—	—

(continued on next page)

Table 1 (continued)

Compd.	R	IC <sub>50</sub> (μM) <sup>a</sup>					
		K <sub>v</sub> 1.1	K <sub>v</sub> 1.2	K <sub>v</sub> 1.3	K <sub>v</sub> 1.4	K <sub>v</sub> 1.5	K <sub>v</sub> 1.6
<b>14b</b>		–	–	n.a.	–	–	–
<b>14c</b>		–	–	n.a.	–	–	–
<b>PAP-1<sup>d</sup></b>		0.25 ± 0.09	0.45 ± 0.06	0.024 ± 0.003	0.17 ± 0.03	0.088 ± 0.022	0.13 ± 0.02

<sup>a</sup> The concentration of compound that inhibits a potassium channel current by 50%. Each IC<sub>50</sub> value is the mean of three independent experiments.

<sup>b</sup> n. a = not active (IC<sub>50</sub> value higher than 30 μM).

<sup>c</sup> Not determined.

<sup>d</sup> 5-(4-Phenoxybutoxy)psoralen.

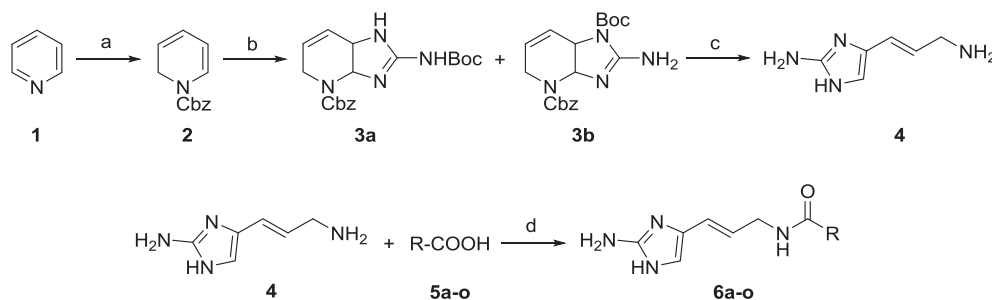


**Fig. 3.** Synthesis of (*E*)-*N*-(3-(2-amino-1*H*-imidazol-4-yl)allyl)carboxamides **6a-o**. Reagents and conditions: (a) benzyl chloroformate, Et<sub>2</sub>O, then NaBH<sub>4</sub>, 2 h, 54%; (b) Br<sub>2</sub>, Et<sub>3</sub>N, *N*-Boc-guanidine, 45 min, 31% (**3a**), 18% (**3b**); (c) 6 M HCl/MeOH, 2 h, 33%; (d) TBTU, NMM, DMF, rt, 6 h, 22–34%.

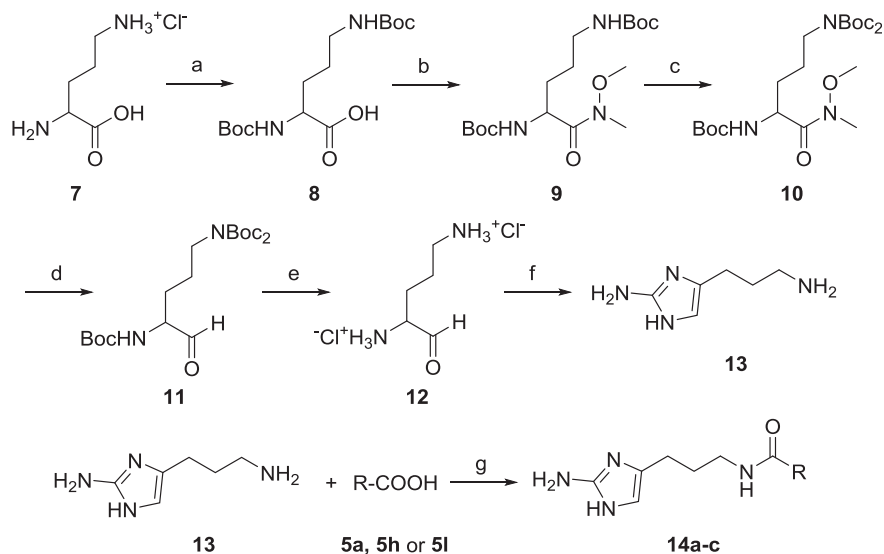


**Fig. 4.** Synthesis of *N*-(3-(2-amino-1*H*-imidazol-4-yl)propyl)carboxamides **14a-c**. Reagents and conditions: (a) Boc<sub>2</sub>O, NaOH, THF/H<sub>2</sub>O, 12 h, 99%; (b) *N*,*O*-dimethylhydroxylamine hydrochloride, Et<sub>3</sub>N, BOP, 2 h, 84%; (c) Boc<sub>2</sub>O, DMAP, MeCN, 24 h, 81%; (d) LiAlH<sub>4</sub>, Et<sub>2</sub>O, 0 °C, 45 min, 67%; (e) HCl<sub>(g)</sub>, Et<sub>2</sub>O, 30 min, 100%; (f) cyanamide, H<sub>2</sub>O, pH 4.5, reflux 3 h, 30%; (g) TBTU, NMM, DMF, rt, 6 h, 58–63%.

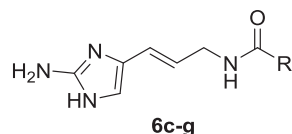
inhibitory activity increased with the introduction of bromo, chloro, or methyl substituents to 3, 4 or 5 positions of the pyrrole ring. Oroidin (**6c**) with 4,5-dibromopyrrole group showed a promising 0.82 μM IC<sub>50</sub> value against K<sub>v</sub>1.3, and 5.7 μM IC<sub>50</sub> value against K<sub>v</sub>1.4 channels. The most potent compounds were **6d**, **6e**, **6f** and **6g** of the type **I** series, for which promising inhibitory activities were obtained against K<sub>v</sub>1.4 channels where they displayed sub-micromolar IC<sub>50</sub> values, i.e. 0.38 μM for **6d**, 0.23 μM for **6e**, 0.73 μM for **6f** and 0.60 μM for **6g**. Like in the patch clamp

experiments, the most potent compound of the series was 4,5-dichloropyrro-2-yl derivative **6g** that, besides displaying the inhibitory activity against K<sub>v</sub>1.4 channels, was also very active against K<sub>v</sub>1.6 channels where 0.17 μM IC<sub>50</sub> value was determined.

In agreement with the results of the patch clamp experiments, in *X. laevis* oocytes compounds with indole (**6h-k**), indolin-2-yl (**6l**), pyridine-3-yl (**6m**), and piperidin-4-yl (**6n-o**) groups on the right-hand side of the molecules were less active than the pyrrole analogues. Only 5-fluoroindole derivative **6i**, and piperidine containing

**Table 2**

Inhibitory activities of five selected (*E*)-*N*-(3-(2-amino-1*H*-imidazol-4-yl)allyl)carboxamides (**6c–g**) on  $K_v1.3$ ,  $K_v1.4$  and  $K_v1.6$  channels expressed in *Xenopus laevis* oocytes.



Compd.	R	IC <sub>50</sub> (μM) <sup>a</sup>		
		$K_v1.3$	$K_v1.4$	$K_v1.6$
<b>6c</b> oroidin		0.82 ± 0.21	5.7 ± 0.8	n.a.
<b>6d</b>		n.a.	0.38 ± 0.09	9.8 ± 1.2
<b>6e</b>		n.a.	0.23 ± 0.04	n.a.
<b>6f</b>		n.a.	0.73 ± 0.05	n.a.
<b>6g</b>		n.a.	0.60 ± 0.12	0.17 ± 0.03

n.a = not active (IC<sub>50</sub> value higher than 10 μM).

<sup>a</sup> The concentration of compound that inhibits a potassium channel current by 50%. Each IC<sub>50</sub> value is the mean of three independent experiments.

analogue **6o** showed weak inhibitory activities against  $K_v1.3$  (28% inhibition at 1 μM) and  $K_v1.1$  (22% inhibition at 1 μM) channels, respectively. Compounds of the type **II** series (**14a–c**) were not active against any of the tested  $K_v1$  isoforms.

In general, the activities of compounds on  $K_v1$  channels expressed in CHO cells and on  $K_v1$  channels expressed in *X. laevis* oocytes were comparable (relative rank order of potencies). Small differences can be explained with potential differences in post-translational modifications of channels because two different expression systems were used. Furthermore, differences in expression of auxiliary subunits might influence kinetics of channel gating [27]. In case of CHO cells the auxiliary β subunits were not co-expressed so  $K_v$  channels might have somewhat different gating characteristics. Moreover, the small differences observed between both test systems can be explained based on the differences in membrane composition together with inherent differences in osmolarity of the recording solutions.

### 3. Conclusion

In recent years, the modulators of voltage-gated potassium channels have received increased scientific attention. Marine natural products represent a viable source of bioactive compounds that modulate the activity of various ion channels. In this study, we have discovered that two alkaloids produced by the *Agelas* sponges, hymenidin and oroidin, inhibit the activity of  $K_v1.3$ ,  $K_v1.4$ ,  $K_v1.5$ ,

and  $K_v1.6$  channels with IC<sub>50</sub> values in the low micromolar range, whereas, clathrocin was found to be inactive across the concentration ranges tested. To probe the SAR, structural modifications of hymenidin and oroidin were prepared represented by 15 analogues, among which, some displayed improved inhibitory activity against  $K_v1.3$ – $K_v1.6$  channels. Two different expression systems were used to express  $K_v1$  channels – CHO cells and *Xenopus laevis* oocytes. The inhibitory activities obtained in two independent test systems were generally in good agreement. The most active natural product analogues were compounds **6d**, **6e**, **6f** and **6g** with (*E*)-4-(3-aminoprop-1-en-1-yl)-1*H*-imidazol-2-amide motif on the left-hand side of the molecules and substituted pyrrol-2-yl group on the right-hand side. 4,5-Dichloropyrro-2-yl derivative **6g** displayed IC<sub>50</sub> values of 1.4 μM, 1.5 μM, and 1.6 μM against  $K_v1.3$ ,  $K_v1.4$ , and  $K_v1.6$  channels respectively in the patch clamp experiments. The same compound displayed and IC<sub>50</sub> of 0.60 μM against  $K_v1.4$  channels and 0.17 μM against  $K_v1.6$  under voltage clamp conditions. Low and sub-micromolar IC<sub>50</sub> values and relatively low molecular weights of the prepared compounds highlight their potential for further optimisation of their inhibitory action against voltage-gated potassium channels.

## 4. Experimental section

### 4.1. Electrophysiology

#### 4.1.1. Automated patch clamp

Chinese Hamster Ovary (CHO) cell lines stably expressing exogenous human α-subunits of  $K_v1.1$ ,  $K_v1.2$ ,  $K_v1.3$  and  $K_v1.4$  were created 'in house' using standard techniques, hKv1.5 was purchased from b-Sys (Switzerland). All cell lines were validated biophysically and pharmacologically on the QPatchHTsystem. Cells were prepared by dissociation from T175 cell culture flasks using trypsin-EDTA (0.05%), cells were kept in serum free media in the cell hotel on board the QPatch HT. These cells were sampled, washed and re-suspended in extracellular recording solution by the QPatch HT immediately before application to well site on the chip. Once in whole-cell configuration vehicle (0.1% DMSO v/v) was applied to the cells as two bolus additions with a 2 min recording period between each addition needed to achieve a stable control recording (4-min total). This was followed by application of four escalating concentrations of test sample applied as double bolus additions per test concentration with 2 min recording time per addition. Currents were elicited from a holding potential of –80 mV with 500 ms activating step to +30 mV applied at a sweep frequency of 0.067 Hz, except  $K_v1.5$  which was activated by 900 ms pulses to 0 mV at a sweep frequency of 0.2 Hz. Series resistance (4–15 MΩ) was compensated by 80% and leak subtraction calculated using a P/n protocol. For each sweep of the voltage protocol charge was calculated as the current integral over time (5–95% duration) during the 500 ms activating test step.

Data was captured using the QPatch assay software (v5.0). The % inhibition was calculated from mean charge over the last three sweeps at the end of each concentration application period relative to that measured at the end of the control period after current stabilisation. Concentration response curves (four parameter logistic curve) were fitted to the % inhibition data using a bioinformatics suite developed running in Pipeline Pilot (Biovia, USA) from which the IC<sub>50</sub> (50% inhibitory concentration) was determined. All data are presented as mean ± SD for a minimum of 3 independent observations.

#### 4.1.2. Two-electrode voltage clamp

For the expression of the VGPCs (rKv1.1, rKv1.2, hKv1.3, rKv1.4, rKv1.5, rKv1.6, hKv10.1) in *Xenopus laevis* oocytes, the linearized

plasmids were transcribed using the T7 or SP6 mMACHINE transcription kit (Ambion, USA). The harvesting of stage V-VI oocytes from anaesthetized female *Xenopus laevis* frog was previously described [28]. Oocytes were injected with 50 nL of cRNA at a concentration of 1 ng/nL using a micro-injector (Drummond Scientific, USA). The oocytes were incubated in a solution containing (in mM): NaCl, 96; KCl, 2; CaCl<sub>2</sub>, 1.8; MgCl<sub>2</sub>, 2 and HEPES, 5 (pH 7.4), supplemented with 50 mg/L gentamicin sulfate.

Two-electrode voltage clamp recordings were performed at room temperature (18–22 °C) using a Geneclamp 500 amplifier (Molecular Devices, USA) controlled by a pClamp data acquisition system (Axon Instruments, USA). Whole cell currents from oocytes were recorded 1–4 days after injection. Bath solution composition was ND96 (in mM): NaCl, 96; KCl, 2; CaCl<sub>2</sub>, 1.8; MgCl<sub>2</sub>, 2 and HEPES, 5 (pH 7.4). Voltage and current electrodes were filled with 3 M KCl. Resistances of both electrodes were kept between 0.8 and 1.5 MΩ. The elicited currents were filtered at 500 Hz and sampled at 1 kHz using a four-pole low-pass Bessel filter. Leak subtraction was performed using a -P/4 protocol. K<sub>v</sub>1 currents were evoked by 500 ms depolarizations to 0 mV followed by a 500 ms pulse to -50 mV, from a holding potential of -90 mV. All data represent at least three independent experiments (n ≥ 3) and are presented as mean ± standard error.

## 4.2. Chemistry—general

Chemicals were obtained from Acros Organics (Geel, Belgium), Sigma-Aldrich (St. Louis, MO, USA) and Apollo Scientific (Stockport, UK) and used without further purification. Analytical TLC was performed on silica gel Merck 60 F<sub>254</sub> plates (0.25 mm), using visualization with UV light and spray reagents. Column chromatography was carried out on silica gel 60 (particle size 240–400 mesh). HPLC analyses were performed on an Agilent Technologies 1100 instrument (Agilent Technologies, Santa Clara, CA, USA) with a G1365B UV–Vis detector, a G1316A thermostat and a G1313A autosampler using a Phenomenex Luna 5-μm C18 column (4.6 × 150 mm or 4.6 × 250 mm, Phenomenex, Torrance, CA, USA) and a flow rate of 1.0 mL/min. The eluent consisted of trifluoroacetic acid (0.1% in water) as solvent A and methanol or acetonitrile as solvent B. Melting points were determined on a Reichert hot stage microscope and are uncorrected. <sup>1</sup>H and <sup>13</sup>C NMR spectra were recorded at 400 and 100 MHz, respectively, on a Bruker AVANCE III 400 spectrometer (Bruker Corporation, Billerica, MA, USA) in DMSO-*d*<sub>6</sub>, MeOH-*d*<sub>4</sub> or CDCl<sub>3</sub> solutions, with TMS as the internal standard. E-configuration was determined measuring corresponding coupling constant [30]. IR spectra were recorded on a Thermo Nicolet Nexus 470 ESP FT-IR spectrometer (Thermo Fisher Scientific, Waltham, MA, USA). Mass spectra were obtained using a VG Analytical Autospec Q mass spectrometer (Fisons, VG Analytical, Manchester, UK). HPLC was used to establish the purity of target compounds. The purity of the tested compounds was established to be ≥ 95%.

## 4.3. Synthetic procedures

Clathrocin (**6a**), hymenidin (**6b**), oroidin (**6c**), and compounds **6h** and **6i** were synthesized as described [26,29].

### 4.3.1. General coupling procedure with TBTU and NMM

The corresponding carboxylic acid (0.36 mmol), TBTU (137 mg, 0.414 mmol) and *N*-methylmorpholine (0.08 mL, 0.72 mmol) were dissolved in dry dimethylformamide (2 mL) and stirred under argon at rt for 1 h. The prepared mixture was added dropwise to a stirred solution of compound **4** or **13** (50 mg, 0.36 mmol) and *N*-methylmorpholine (0.08 mL, 0.72 mmol) in dry

dimethylformamide (1 mL) at 0 °C. After 1 h, the mixture was warmed to rt and stirred under argon for 5 h. The solvent was evaporated under reduced pressure, and the residue was purified by flash column chromatography using dichloromethane/methanol saturated with NH<sub>3</sub> (6:1) as an eluent.

4.3.1.1. (*E*)-*N*-(3-(2-amino-1*H*-imidazol-4-yl)allyl)-4-bromo-5-methyl-1*H*-pyrrole-2-carboxamide (**6d**). Synthesized from **13** (45 mg, 0.326 mmol) and 4-bromo-5-methyl-1*H*-pyrrole-2-carboxylic acid (67 mg, 0.326 mmol) using general coupling procedure with TBTU and NMM. Yield: 35 mg (33%) as white solid; m. p.: 124–127 °C; IR (ATR):  $\nu = 3214, 2918, 2851, 1615, 1573, 1528, 1480, 1417, 1328, 1267, 1215, 1098, 1049, 1023, 957, 805, 717, 629 \text{ cm}^{-1}$ ; <sup>1</sup>H NMR (MeOH-*d*<sub>4</sub>, 400 MHz): 2.23 (s, 3H, -CH<sub>3</sub>), 4.02 (dd, 2H, *J* = 6.1 Hz, *J* = 1.3 Hz, -CH=CH-CH<sub>2</sub>-), 5.90 (td, 1H, *J* = 15.7 Hz, *J* = 6.1 Hz, -CH=CH-CH<sub>2</sub>-), 6.30 (td, 1H, *J* = 15.8 Hz, *J* = 1.3 Hz, -CH=CH-CH<sub>2</sub>-), 6.48 (s, 1H, imidazole-H), 6.75 (s, 1H, pyrrole-H) ppm; <sup>13</sup>C NMR (MeOH-*d*<sub>4</sub>, 100 MHz): 162.59, 151.97, 131.45, 125.34, 122.49, 121.79, 117.65, 113.57, 96.67, 49.73, 42.14, 11.39 ppm; HRMS (C<sub>12</sub>H<sub>14</sub>BrN<sub>5</sub>O): calculated (MH<sup>+</sup>) 324.0460; found (MH<sup>+</sup>) 324.0458.

4.3.1.2. (*E*)-*N*-(3-(2-amino-1*H*-imidazol-4-yl)allyl)-3,4-dibromo-5-methyl-1*H*-pyrrole-2-carboxamide (**6e**). Synthesized from **4** (40 mg, 0.289 mmol) and 3,4-dibromo-5-methyl-1*H*-pyrrole-2-carboxylic acid (82 mg, 0.289 mmol) using general coupling procedure with TBTU and NMM. Yield: 36 mg (30%) as white-yellow solid; m. p.: 123–126 °C; IR (ATR):  $\nu = 3396, 3191, 2924, 1620, 1528, 1475, 1371, 1264, 1166, 1062, 957, 760, 708 \text{ cm}^{-1}$ ; <sup>1</sup>H NMR (MeOH-*d*<sub>4</sub>, 400 MHz): 2.28 (s, 3H, -CH<sub>3</sub>), 4.11 (dd, 2H, *J* = 6.1 Hz, *J* = 1.3 Hz, -CH=CH-CH<sub>2</sub>-), 5.93 (td, 1H, *J* = 15.7 Hz, *J* = 6.0 Hz, -CH=CH-CH<sub>2</sub>-), 6.36 (td, 1H, *J* = 15.8 Hz, *J* = 1.3 Hz, -CH=CH-CH<sub>2</sub>-), 6.50 (s, 1H, imidazole-H) ppm; <sup>13</sup>C NMR (MeOH-*d*<sub>4</sub>, 100 MHz): 161.25, 152.13, 131.94, 123.22, 123.18, 122.72, 120.99, 100.94, 100.54, 49.87, 42.33, 12.16 ppm; HRMS (C<sub>12</sub>H<sub>13</sub>Br<sub>2</sub>N<sub>5</sub>O): calculated (MH<sup>+</sup>) 401.9565; found (MH<sup>+</sup>) 401.9562.

4.3.1.3. (*E*)-*N*-(3-(2-amino-1*H*-imidazol-4-yl)allyl)-4-chloro-5-methyl-1*H*-pyrrole-2-carboxamide (**6f**). Synthesized from **4** (60 mg, 0.435 mmol) and 4-chloro-5-methyl-1*H*-pyrrole-2-carboxylic acid (69 mg, 0.435 mmol) using general coupling procedure with TBTU and NMM. Yield: 36 mg (30%) as a yellow solid; m. p.: 125–127 °C; IR (ATR):  $\nu = 3210, 2919, 1614, 1577, 1529, 1484, 1419, 1330, 1269, 1218, 1164, 1073, 1026, 957, 808, 753, 688 \text{ cm}^{-1}$ ; <sup>1</sup>H NMR (MeOH-*d*<sub>4</sub>, 400 MHz): 2.22 (s, 3H, -CH<sub>3</sub>), 4.02 (dd, 2H, *J* = 6.1 Hz, *J* = 1.3 Hz, -CH=CH-CH<sub>2</sub>-), 5.89 (m, 1H, -CH=CH-CH<sub>2</sub>-), 6.30 (td, 1H, *J* = 15.8 Hz, *J* = 1.3 Hz, -CH=CH-CH<sub>2</sub>-), 6.47 (s, 1H, imidazole-H), 6.68 (s, 1H, pyrrole-H) ppm; <sup>13</sup>C NMR (MeOH-*d*<sub>4</sub>, 100 MHz): 162.70, 152.07, 129.49, 124.14, 122.68, 121.57, 111.23, 111.00, 49.73, 42.16, 10.38 ppm; HRMS (C<sub>12</sub>H<sub>14</sub>ClN<sub>5</sub>O): calculated (MH<sup>+</sup>) 280.0965; found (MH<sup>+</sup>) 280.0959.

4.3.1.4. (*E*)-*N*-(3-(2-amino-1*H*-imidazol-4-yl)allyl)-4,5-dichloro-1*H*-pyrrole-2-carboxamide (**6g**). Synthesized from **4** (50 mg, 0.357 mmol) and 4,5-dichloro-1*H*-pyrrole-2-carboxylic acid (64 mg, 0.357 mmol) using general coupling procedure with TBTU and NMM. Yield: 37 mg (35%) as white-yellow solid; m. p.: 75–77 °C; IR (ATR):  $\nu = 3370, 3152, 1688, 1613, 1567, 1525, 1433, 1329, 1246, 1017, 958, 825, 757, 627 \text{ cm}^{-1}$ ; <sup>1</sup>H NMR (MeOH-*d*<sub>4</sub>, 400 MHz): 4.04 (dd, 2H, *J* = 6.0 Hz, *J* = 1.2 Hz, -CH=CH-CH<sub>2</sub>-), 5.97 (td, 1H, *J* = 15.9 Hz, *J* = 6.0 Hz, -CH=CH-CH<sub>2</sub>-), 6.31 (td, 1H, *J* = 15.8 Hz, *J* = 1.2 Hz, -CH=CH-CH<sub>2</sub>-), 6.59 (s, 1H, imidazole-H), 6.79 (s, 1H, pyrrole-H) ppm; HRMS (C<sub>11</sub>H<sub>11</sub>Cl<sub>2</sub>N<sub>5</sub>O): calculated (MH<sup>+</sup>) 300.0419; found (MH<sup>+</sup>) 300.0420.

4.3.1.5. (*E*)-*N*-(3-(2-amino-1*H*-imidazol-4-yl)allyl)-5-chloro-1*H*-indole-2-carboxamide (**6j**). Synthesized from **4** (50 mg, 0.357 mmol) and 5-chloro-1*H*-indole-2-carboxylic acid (70 mg, 0.357 mmol) using general coupling procedure with TBTU and NMM. Yield: 40 mg (36%) as yellow solid; m. p.: 149–152 °C; IR (ATR):  $\nu = 3230, 2923, 1618, 1541, 1475, 1416, 1319, 1283, 1253, 1210, 1165, 1126, 1060, 957, 917, 867, 799, 732, 653 \text{ cm}^{-1}$ ;  $^1\text{H NMR}$  (MeOH- $d_4$ , 400 MHz): 4.11 (dd, 2H,  $J = 6.2 \text{ Hz}, J = 1.3 \text{ Hz}$ , -CH=CH-CH $_2$ -), 5.95 (td, 1H,  $J = 15.8 \text{ Hz}, J = 6.1 \text{ Hz}$ , -CH=CH-CH $_2$ -), 6.36 (td, 1H,  $J = 15.8 \text{ Hz}, J = 1.3 \text{ Hz}$ , -CH=CH-CH $_2$ -), 6.50 (s, 1H, imidazole-H), 7.06 (d, 1H,  $J = 0.9 \text{ Hz}$ , indole-H), 7.19 (dd, 1H,  $J = 8.8 \text{ Hz}, J = 2.1 \text{ Hz}$ , indole-H), 7.42–7.45 (m, 1H, indole-H), 7.61 (dd, 1H,  $J = 2.0 \text{ Hz}, J = 0.6 \text{ Hz}$ , indole-H) ppm;  $^{13}\text{C NMR}$  (MeOH- $d_4$ , 100 MHz): 162.04, 150.59, 135.16, 132.44, 128.57, 125.31, 123.80, 121.45, 120.41, 119.99, 116.30, 112.99, 102.26, 48.10, 41.04 ppm.; HRMS (C $_{15}$ H $_{14}$ ClN $_5$ O): calculated (MH $^+$ ) 316.0965; found (MH $^+$ ) 316.0961.

4.3.1.6. (*E*)-*N*-(3-(2-amino-1*H*-imidazol-4-yl)allyl)-5-methoxy-1*H*-indole-2-carboxamide (**6k**). Synthesized from **4** (60 mg, 0.435 mmol) and 5-methoxy-1*H*-indole-2-carboxylic acid (83 mg, 0.435 mmol) using general coupling procedure with TBTU and NMM. Yield: 47 mg (35%) as orange solid; m. p.: 125–128 °C; IR (ATR):  $\nu = 3239, 2936, 1617, 1541, 1482, 1450, 1417, 1376, 1331, 1225, 1161, 1119, 1024, 957, 840, 800, 763, 733, 669 \text{ cm}^{-1}$ ;  $^1\text{H NMR}$  (MeOH- $d_4$ , 400 MHz): 3.83 (s, 3H, -OCH $_3$ ), 4.11 (dd, 2H,  $J = 6.1 \text{ Hz}, J = 1.3 \text{ Hz}$ , -CH=CH-CH $_2$ -), 5.95 (td, 1H,  $J = 15.9 \text{ Hz}, J = 6.0 \text{ Hz}$ , -CH=CH-CH $_2$ -), 6.36 (td, 1H,  $J = 15.8 \text{ Hz}, J = 1.3 \text{ Hz}$ , -CH=CH-CH $_2$ -), 6.50 (s, 1H, imidazole-H), 6.90 (dd, 1H,  $J = 8.9 \text{ Hz}, J = 2.5 \text{ Hz}$ , indole-H), 7.03 (d, 1H,  $J = 0.9 \text{ Hz}$ , indole-H), 7.08 (d, 1H,  $J = 2.1 \text{ Hz}$ , indole-H), 7.33–7.36 (m, 1H, indole-H) ppm;  $^{13}\text{C NMR}$  (MeOH- $d_4$ , 100 MHz): 163.95, 155.85, 151.97, 133.68, 132.59, 129.34, 122.69, 121.65, 116.42, 113.89, 104.18, 103.12, 56.05, 49.85, 42.40 ppm; HRMS (C $_{16}$ H $_{17}$ N $_5$ O $_2$ ): calculated (MH $^+$ ) 312.1461; found (MH $^+$ ) 312.1465.

4.3.1.7. (*E*)-*N*-(3-(2-amino-1*H*-imidazol-4-yl)allyl)-indoline-2-carboxamide (**6l**). Synthesized from **4** (83 mg, 0.602 mmol) and indoline-2-carboxylic acid (115 mg, 0.602 mmol) using general coupling procedure with TBTU and NMM. Yield: 50 mg (27%) as white solid; m. p.: 79–82 °C; IR (ATR):  $\nu = 3328, 2915, 1638, 1578, 1526, 1483, 1465, 1245, 1097, 958, 743 \text{ cm}^{-1}$ ;  $^1\text{H NMR}$  (DMSO- $d_6$ , 400 MHz): 2.90 (dd, 1H,  $J = 16.0 \text{ Hz}, J = 8.8 \text{ Hz}$ , -NHCHCH $_2$ -), 3.36 (dd, 1H,  $J = 16.0 \text{ Hz}, J = 10.5 \text{ Hz}$ , -NHCHCH $_2$ -), 3.59 (dd, 2H,  $J = 6.2 \text{ Hz}, J = 1.3 \text{ Hz}$ , -CH=CH-CH $_2$ -), 4.01 (m, 1H, -NHCHCH $_2$ -), 5.71 (m, 1H, -CH=CH-CH $_2$ -), 6.09 (d, 1H,  $J = 15.6 \text{ Hz}$ , -CH=CH-CH $_2$ -), 6.50 (s, 1H, imidazole-H), 6.61–6.65 (m, 2H, indoline-H), 6.99 (t, 1H,  $J = 5.51$ , -CONH-), 7.12–7.18 (m, 2H, indoline-H) ppm; HRMS (C $_{15}$ H $_{18}$ N $_5$ O): calculated (MH $^+$ ) 284.1511; found (MH $^+$ ) 284.1510.

4.3.1.8. (*E*)-*N*-(3-(2-amino-1*H*-imidazol-4-yl)allyl)nicotinamide (**6m**). Synthesized from **4** (50 mg, 0.357 mmol) and nicotinic acid (44 mg, 0.357 mmol) using general coupling procedure with TBTU and NMM. Yield: 22 mg (24%) as a white solid; m. p.: 81–83 °C; IR (ATR):  $\nu = 3219, 2925, 163, 1591, 1539, 1474, 1418, 1308, 1197, 1161, 1027, 958, 825, 703, 627 \text{ cm}^{-1}$ ;  $^1\text{H NMR}$  (MeOH- $d_4$ , 400 MHz): 4.12 (dd, 2H,  $J = 6.3 \text{ Hz}, J = 1.3 \text{ Hz}$ , -CH=CH-CH $_2$ -), 5.95 (td, 1H,  $J = 15.8 \text{ Hz}, J = 6.0 \text{ Hz}$ , -CH=CH-CH $_2$ -), 6.36 (td, 1H,  $J = 15.8 \text{ Hz}, J = 1.2 \text{ Hz}$ , -CH=CH-CH $_2$ -), 6.51 (s, 1H, imidazole-H), 6.57 (ddd, 1H,  $J = 8.0 \text{ Hz}, J = 4.9 \text{ Hz}, J = 0.9 \text{ Hz}$ , pyridine-H), 8.28 (ddd, 1H,  $J = 8.0 \text{ Hz}, J = 2.3 \text{ Hz}, J = 1.7 \text{ Hz}$ , pyridine-H), 8.70 (dd, 1H,  $J = 4.9 \text{ Hz}, J = 1.6 \text{ Hz}$ , pyridine-H), 9.01 (dd, 1H,  $J = 2.3 \text{ Hz}, J = 0.9 \text{ Hz}$ , pyridine-H) ppm;  $^{13}\text{C NMR}$  (MeOH- $d_4$ , 100 MHz): 167.51, 152.63, 152.06, 149.17, 137.06, 132.08, 125.18, 123.32, 120.99, 117.61, 49.73, 43.02 ppm; HRMS (C $_{12}$ H $_{13}$ N $_5$ O): calculated (MH $^+$ ) 244.1198; found

(MH $^+$ ) 244.1202.

4.3.1.9. *tert*-butyl (*E*)-4-((3-(2-amino-1*H*-imidazol-4-yl)allyl)carbamoyl)piperidine-1-carboxylate (**6n**). Synthesized from **4** (55 mg, 0.393 mmol) and 1-(*tert*-butoxycarbonyl)piperidine-4-carboxylic acid (91 mg, 0.393 mmol) using general coupling procedure with TBTU and NMM. Yield: 53 mg (37%) as brown solid; m. p.: 98–101 °C; IR (ATR):  $\nu = 3310, 2929, 2858, 1646, 1579, 1536, 1424, 1365, 1322, 1221, 957 \text{ cm}^{-1}$ ;  $^1\text{H NMR}$  (DMSO- $d_5$ , 400 MHz): 1.42 (s, 9H, (CH $_3$ ) $_3$ ), 2.08–2.18 (m, 2H, piperidine-CH $_2$ -), 2.32–2.38 (m, 2H, piperidine-CH $_2$ -), 2.73–2.79 (m, 1H, piperidine-CH-), 3.49–3.53 (m, 2H, piperidine-CH $_2$ -), 3.81–3.86 (m, 2H, piperidine-CH $_2$ -), 3.93 (dd, 2H,  $J = 6.0 \text{ Hz}, J = 1.3 \text{ Hz}$ , -CH=CH-CH $_2$ -), 6.02 (td, 1H,  $J = 16.0 \text{ Hz}, J = 6.0 \text{ Hz}$ , -CH=CH-CH $_2$ -), 6.31 (dd, 1H,  $J = 16.0 \text{ Hz}, J = 1.5 \text{ Hz}$ , -CH=CH-CH $_2$ -), 6.82 (s, 1H, imidazole-H) ppm; HRMS (C $_{17}$ H $_{28}$ N $_5$ O $_3$ ): calculated (MH $^+$ ) 350.2192; found (MH $^+$ ) 350.2197.

4.3.1.10. (*E*)-*N*-(3-(2-amino-1*H*-imidazol-4-yl)allyl)piperidine-4-carboxamide (**6o**). Synthesized from **6n** (27 mg, 0.077 mmol) by Boc deprotection in HCl/EtOH. Yield: 13 mg (66%) as brown solid; m. p.: 43–45 °C; IR (ATR):  $\nu = 3259, 2925, 2852, 2499, 1636, 1542, 1451, 1301, 1239, 1075, 1004, 958 \text{ cm}^{-1}$ ;  $^1\text{H NMR}$  (MeOH- $d_4$ , 400 MHz): 1.87–1.97 (m, 2H, piperidine-CH $_2$ -), 2.02–2.07 (m, 2H, piperidine-CH $_2$ -), 2.59–2.65 (m, 1H, piperidine-CH-), 3.03–3.10 (m, 2H, piperidine-CH $_2$ -), 3.43–3.47 (m, 2H, piperidine-CH $_2$ -), 3.94 (dd, 2H,  $J = 6.0 \text{ Hz}, J = 1.3 \text{ Hz}$ , -CH=CH-CH $_2$ -), 6.01 (td, 1H,  $J = 16.0 \text{ Hz}, J = 6.0 \text{ Hz}$ , -CH=CH-CH $_2$ -), 6.31 (ddd, 1H,  $J = 16.0 \text{ Hz}, J = 1.5 \text{ Hz}, J = 1.1 \text{ Hz}$ , -CH=CH-CH $_2$ -), 6.71 (s, 1H, imidazole-H) ppm;  $^{13}\text{C NMR}$  (MeOH- $d_4$ , 100 MHz): 174.35, 148.63, 126.85, 124.27, 118.06, 112.10, 73.00, 51.89, 43.00, 40.51, 39.60, 25.38 ppm; HRMS (C $_{12}$ H $_{19}$ N $_5$ O): calculated (MH $^+$ ) 250.1668; found (MH $^+$ ) 250.1667.

4.3.1.11. *N*-(3-(2-amino-1*H*-imidazol-4-yl)propyl)-4,5-dibromo-1*H*-pyrrole-2-carboxamide (**14a**). Synthesized from **13** (40 mg, 0.286 mmol) and 4,5-dibromo-1*H*-pyrrole-2-carboxylic acid (77 mg, 0.286 mmol) using general coupling procedure with TBTU and NMM. Yield: 56 mg (51%) as white crystals; m. p.: 68–70 °C; IR (ATR):  $\nu = 3481, 3381, 3121, 2938, 1689, 1644, 1561, 1510, 1429, 1414, 1367, 1316, 1235, 1055, 1014, 973, 830, 780, 651 \text{ cm}^{-1}$ ;  $^1\text{H NMR}$  (MeOH- $d_4$ , 400 MHz): 1.85 (p, 2H,  $J = 7.2 \text{ Hz}$ , -CH $_2$ CH $_2$ CH $_2$ NH-), 2.51 (t, 2H,  $J = 7.7 \text{ Hz}$ , -CH $_2$ CH $_2$ CH $_2$ NH-), 3.35–3.37 (m, 2H, -CH $_2$ CH $_2$ CH $_2$ NH-), 6.37 (s, 1H, imidazole-H), 6.82 (s, 1H, pyrrole-H) ppm;  $^{13}\text{C NMR}$  (MeOH- $d_4$ , 100 MHz): 161.91, 149.95, 132.21, 128.97, 114.17, 111.26, 106.11, 99.87, 39.89, 30.03, 24.52 ppm; HRMS (C $_{11}$ H $_{13}$ Br $_2$ N $_5$ O): calculated (MH $^+$ ) 389.9565; found (MH $^+$ ) 389.9559.

4.3.1.12. *N*-(3-(2-amino-1*H*-imidazol-4-yl)propyl)-1*H*-indole-2-carboxamide (**14b**). Synthesized from **13** (53 mg, 0.378 mmol) and indole-2-carboxylic acid (61 mg, 0.378 mmol) using general coupling procedure with TBTU and NMM. Yield: 63 mg (59%) as white crystals; m. p.: 76–78 °C; IR (ATR):  $\nu = 3617, 3392, 2868, 2567, 1679, 1616, 1553, 1493, 1429, 1417, 1340, 1308, 1257, 1035, 745 \text{ cm}^{-1}$ ;  $^1\text{H NMR}$  (DMSO- $d_6$ , 400 MHz): 1.80 (m, 2H, -CH $_2$ CH $_2$ CH $_2$ NH-), 2.51 (m, 2H, -CH $_2$ CH $_2$ CH $_2$ NH-), 3.36–3.38 (m, 2H, -CH $_2$ CH $_2$ CH $_2$ NH-), 6.39 (s, 1H, imidazole-H), 6.89 (s, 1H, pyrrole-H) ppm; HRMS (C $_{15}$ H $_{18}$ N $_5$ O): calculated (MH $^+$ ) 284.1511; found (MH $^+$ ) 284.1505.

4.3.1.13. *N*-(3-(2-amino-1*H*-imidazol-4-yl)propyl)indoline-2-carboxamide (**14c**). Synthesized from **13** (35 mg, 0.250 mmol) and indoline-2-carboxylic acid (41 mg, 0.250 mmol) using general coupling procedure with TBTU and NMM. Yield: 37 mg (53%) as white crystals; m. p.: 67–69 °C; IR (ATR):  $\nu = 3306, 2926, 1640, 1607, 1560, 1531, 1484, 1466, 1245, 1104, 1057, 1018, 996, 883, 744,$

632, 602  $\text{cm}^{-1}$ ;  $^1\text{H}$  NMR (MeOH- $d_4$ , 400 MHz): 1.78 (p, 2H,  $J = 7.1$  Hz,  $-\text{CH}_2\text{CH}_2\text{CH}_2\text{NH}-$ ), 2.45 (t, 2H,  $J = 7.7$  Hz,  $-\text{CH}_2\text{CH}_2\text{CH}_2\text{NH}-$ ), 2.97 (dd, 1H,  $J = 16.0$  Hz,  $J = 8.9$  Hz,  $-\text{NHCHCH}_2-$ ), 3.27–3.30 (m, 2H,  $-\text{CH}_2\text{CH}_2\text{CH}_2\text{NH}$ ), 3.47 (dd, 1H,  $J = 16.0$  Hz,  $J = 10.5$  Hz,  $-\text{NHCHCH}_2-$ ), 6.27 (s, 1H, imidazole-H), 6.69–6.73 (m, 2H, indoline-H), 6.99–7.06 (m, 2H, indoline-H) ppm;  $^{13}\text{C}$  NMR (MeOH- $d_4$ , 100 MHz): 177.19, 151.93, 150.50, 133.57, 128.78, 128.57, 125.35, 120.57, 111.70, 111.43, 62.62, 39.72, 36.49, 29.99, 25.14 ppm; HRMS ( $\text{C}_{15}\text{H}_{19}\text{N}_5\text{O}$ ): calculated ( $\text{MH}^+$ ) 286.1668; found ( $\text{MH}^+$ ) 286.1662.

#### 4.4. Screening against PAINS

To evaluate a library of the synthesized compounds against PAINS, all tested compounds were screened against the PAINS filter as available in Schrödinger Release 2016–3: Canvas, version 2.9, Schrödinger, LLC, New York, NY, 2016, was used. All compounds passed the PAINS filter.

#### Author contributions

The manuscript was written through contributions of all authors. All authors have given approval to the final version of the manuscript.

#### Conflict of interest

The authors declare no conflict of interest including any financial, personal or other relationships with other people or organizations.

#### Acknowledgement

This work was supported by the Slovenian Research Agency (Grant No. P1-0208 and Grant No. Z1-5458) and by the EU FP7 Integrated Project MAREX (Project No. FP7-KBBE-2009-3-245137). J.T. was supported in part by FWO-Vlaanderen grant G.0E34.14, IUAP 7/10 (Inter-University Attraction Poles Program, Belgian State, Belgian Science Policy) and OT/12/081 (KU Leuven). The authors thank Janja Belinc and Samo Jakovac for the help with voltage-clamp electrophysiology, and Dr. Dušan Žigon (Mass Spectrometry Center, Jožef Stefan Institute, Ljubljana, Slovenia) for recording the mass spectra.

#### Appendix A. Supplementary data

Supplementary data related to this article can be found at <http://dx.doi.org/10.1016/j.ejmech.2017.08.015>.

#### Abbreviations

4-AP	4-aminopyridine
Boc	<i>tert</i> -butyloxycarbonyl
BOB	(benzotriazol-1-yloxy)tris(dimethylamino)phosphonium hexafluorophosphate
CHO cells	Chinese hamster ovary cells
DMF	<i>N,N</i> -dimethylformamide
CRAC	calcium release-activated channels
ESI	electrospray ionization
$\text{K}_v$ channel	voltage-gated potassium channel
NMM	<i>N</i> -methylmorpholine
TBA	Tetrabutylammonium
TBTU	<i>N,N,N',N'</i> -tetramethyl- <i>O</i> -(benzotriazol-1-yl)uronium tetrafluoroborate
TFA	trifluoroacetic acid
THF	tetrahydrofuran

#### References

- [1] G. Yellen, The voltage-gated potassium channels and their relatives, *Nature* 419 (2002) 35–42.
- [2] G.A. Gutman, K.G. Chandy, S. Grissmer, M. Lazdunski, D. Mckinnon, L.A. Pardo, G.A. Robertson, B. Rudy, M.C. Sanguinetti, W. Stuhmer, X.L. Wang, International Union of Pharmacology. LIII. Nomenclature and molecular relationships of voltage-gated potassium channels, *Pharmacol. Rev.* 57 (2005) 473–508.
- [3] N.A. Castle, Pharmacological modulation of voltage-gated potassium channels as a therapeutic strategy, *Expert Opin. Ther. Pat.* 20 (2010) 1471–1503.
- [4] H. Wulff, N.A. Castle, L.A. Pardo, Voltage-gated potassium channels as therapeutic targets, *Nat. Rev. Drug Discov.* 8 (2009) 982–1001.
- [5] D. Daly, A. Al-Sabi, G.K. Kinsella, K. Nolan, J.O. Dolly, Porphyrin derivatives as potent and selective blockers of neuronal  $\text{K}_v$  channels, *Chem. Commun. (Camb)* 51 (2015) 1066–1069.
- [6] S.J. Wacker, W. Jurkowski, K.J. Simmons, C.W.G. Fishwick, A.P. Johnson, D. Madge, E. Lindahl, J.F. Rolland, B.L. de Groot, Identification of selective inhibitors of the potassium channel  $\text{Kv}1.1$ - $1.2(3)$  by high-throughput virtual screening and automated patch clamp, *ChemMedChem* 7 (2012) 1775–1783.
- [7] J.K. Murray, Y.X. Qian, B.X. Liu, R. Elliott, J. Aral, C. Park, X.X. Zhang, M. Stenkilsson, K. Salyers, M. Rose, H.Y. Li, S. Yu, K.L. Andrews, A. Colombero, J. Werner, K. Gaida, E.A. Sickmier, P. Miu, A. Itano, J. McGivern, C.V. Gegg, J.K. Sullivan, L.P. Miranda, Pharmaceutical optimization of peptide toxins for ion channel targets: potent, selective, and long-lived antagonists of  $\text{Kv}1.3$ , *J. Med. Chem.* 58 (2015) 6784–6802.
- [8] S.C. Chang, R. Huq, S. Chhabra, C. Beeton, M.W. Pennington, B.J. Smith, R.S. Norton, N-terminally extended analogues of the  $\text{K}^+$  channel toxin from *Stichodactyla helianthus* as potent and selective blockers of the voltage-gated potassium channel  $\text{Kv}1.3$ , *FEBS J.* 282 (2015) 2247–2259.
- [9] M.W. Pennington, S.C. Chang, S. Chauhan, R. Huq, R.B. Tajhya, S. Chhabra, R.S. Norton, C. Beeton, Development of highly selective  $\text{Kv}1.3$ -blocking peptides based on the sea anemone peptide ShK, *Mar. Drugs* 13 (2015) 529–542.
- [10] N. Vonderlin, F. Fischer, E. Zitron, C. Seyler, D. Scherer, D. Thomas, H.A. Katus, E.P. Scholz, Inhibition of cardiac  $\text{Kv}1.5$  potassium current by the anesthetic midazolam: mode of action, *Drug Des. Dev. Ther.* 8 (2014) 2263–2271.
- [11] F. Fischer, N. Vonderlin, E. Zitron, C. Seyler, D. Scherer, R. Becker, H.A. Katus, E.P. Scholz, Inhibition of cardiac  $\text{Kv}1.5$  and  $\text{Kv}4.3$  potassium channels by the class Ia anti-arrhythmic ajmaline: mode of action, *N-S Arch. Pharmacol.* 386 (2013) 991–999.
- [12] J. Tamargo, R. Caballero, R. Gomez, E. Delpon, I-Kur/ $\text{Kv}1.5$  channel blockers for the treatment of atrial fibrillation, *Expert Opin. Inv Drug* 18 (2009) 399–416.
- [13] M.D. Cahalan, K.G. Chandy, The functional network of ion channels in T lymphocytes, *Immunol. Rev.* 231 (2009) 59–87.
- [14] C. Jorgensen, L. Darre, K. Vanommeslaeghe, K. Omoto, D. Pryde, C. Domene, In silico identification of PAP-1 binding sites in the  $\text{Kv}1.2$  potassium channel, *Mol. Pharm.* 12 (2015) 1299–1307.
- [15] G.C. Koo, et al., Correolide and derivatives are novel immunosuppressants blocking the lymphocyte  $\text{Kv}1.3$  potassium channels, *Cell Immunol.* 197 (1999) 99–107.
- [16] A. Schmitz, et al., Design of PAP-1, a selective small molecule  $\text{Kv}1.3$  blocker, for the suppression of effector memory T cells in autoimmune diseases, *Mol. Pharmacol.* 68 (2005) 1254–1270.
- [17] S.B. Long, E.B. Campbell, R. MacKinnon, Voltage sensor of  $\text{Kv}1.2$ : structural basis of electromechanical coupling, *Science* 309 (2005) 903–908.
- [18] X.R. Chen, Q.H. Wang, F.Y. Ni, J.P. Ma, Structure of the full-length Shaker potassium channel  $\text{Kv}1.2$  by normal-mode-based X-ray crystallographic refinement, *P Natl. Acad. Sci. USA.* 107 (2010) 11352–11357.
- [19] A.N. Miller, S.B. Long, Crystal structure of the human two-pore domain potassium channel  $\text{K}2\text{P}1$ , *Science* 335 (2012) 432–436.
- [20] P. Kiuru, M.V. D'Auria, C.D. Muller, P. Tammela, H. Vuorela, J. Yli-Kauhaluoma, Exploring marine resources for bioactive compounds, *Planta Med.* 80 (2014) 1234–1246.
- [21] S. Peigneur, A. Žula, N. Zidar, F. Chan-Porter, R. Kirby, D. Madge, J. Ilaš, D. Kikelj, J. Tytgat, Action of clathrocin and analogues on voltage-gated sodium channels, *Mar. Drugs* 12 (2014) 2132–2143.
- [22] Z. Hodnik, T. Tomašič, L.P. Mašič, F. Chan, R.W. Kirby, D.J. Madge, D. Kikelj, Novel state-dependent voltage-gated sodium channel modulators, based on marine alkaloids from *Agelas* sponges, *Eur. J. Med. Chem.* 70 (2013) 154–164.
- [23] A.L.R. Rentas, R. Rosa, A.D. Rodriguez, G.E. Demotta, Effect of alkaloid toxins from tropical marine sponges on membrane sodium currents, *Toxicol* 33 (1995) 491–497.
- [24] H. Kim, I. Yang, S.Y. Ryu, D.H. Won, A.G. Giri, W. Wang, H. Choi, J. Chin, D. Hahn, E. Kim, C. Han, J. Lee, S.J. Nam, W.K. Ho, H. Kang, Acreidinones A and B, voltage-dependent potassium channel inhibitors from the sponge-derived fungus *Acremonium* sp F9A015, *J. Nat. Prod.* 78 (2015) 363–367.
- [25] V. Martin, C. Vale, S. Bondu, O.P. Thomas, M.R. Vieytes, L.M. Botana, Differential effects of crambescins and crambescidin 816 in voltage-gated sodium, potassium and calcium channels in neurons, *Chem. Res. Toxicol.* 26 (2013) 169–178.
- [26] A. Žula, D. Kikelj, J. Ilaš, A convenient strategy for synthesizing the *Agelas* alkaloids clathrocin, oroidin, and hymenidin and their (un)saturated linker analogs, *Tetrahedron Lett.* 55 (2014) 3999–4001.
- [27] V.N. Uebele, S.K. England, A. Chaudhary, M.M. Tamkun, D.J. Snyders, Functional differences in  $\text{Kv}1.5$  currents expressed in mammalian cell lines are due

- to the presence of endogenous Kv beta 2.1 subunits, *J. Biol. Chem.* 271 (1996) 2406–2412.
- [28] E.R. Liman, J. Tytgat, P. Hess, Subunit Stoichiometry of a Mammalian K<sup>+</sup> Channel determined by construction of multimeric cDNAs, *Neuron* 9 (1992) 861–871.
- [29] N. Židar, S. Montalvão, Z. Hodnik, D.A. Nawrot, A. Žula, J. Ilaš, D. Kikelj, P. Tammela, L.P. Mašič, Antimicrobial activity of the marine alkaloids, clathrocin and oroidin, and their synthetic analogues, *Mar. Drugs* 12 (2014) 940–963.
- [30] T. Lindel, M. Hochgürtel, Synthesis of the marine natural product oroidin and its Z-isomer, *J. Org. Chem.* 65 (2000) 2806–2809.